Journal of Solid State Chemistry **147,** 372–378 (1999)
Article ID jssc.1999.8374, available online at http://www.idealibrary.com on IDEAL®

$La_4[(C_2)_{1-x}Ge_x]_3$, Lanthanum(III) Dicarbide(4-) Germanide(4-) Mixed Crystals: A Continuous Transition between the Cubic Structure Types *cI*40 (Rb_4O_6/Pu_2C_3) and *cI*28 (Th_3P_4)

Wilder Carrillo-Cabrera,[1] Jan Curda, Karl Peters, and Hans Georg von Schnering[2]

Max-Planck-Institut für Festkörperforschung, Heisenbergstraße 1, D-70569 Stuttgart, Germany

Received January 20, 1999; in revised form April 26, 1999; accepted May 10, 1999

IN MEMORIAM PROFESSOR JEAN ROUXEL

$La_4(C_2)_2Ge$ was obtained as a minor component from the reaction of the elements in corundum crucibles enclosed in stainless steel ampoules at 1360 K. The compound is gray with metallic luster. The crystal structure (space group $I\bar{4}3d$ (No. 220); $a = 8.995(1)$ Å; $Z = 4$; $R(F) = 0.033$, $R_w(F^2) = 0.061$ for 106 reflections (all data) with $2\theta_{max} = 50^\circ$ measured on four-circle diffractometer) may be described as a 3D framework of condensed La_8 dodecahedra (bisdisphenoids) centered by Ge atoms and C_2 dumbbells (d(C–C) = 1.22 Å). $La_4(C_2)_2Ge$ and the previous reported cubic compounds $La_2C_3 \triangleq La_4(C_2)_3$, "$La_5C_{1.5}Ge_3$" $\triangleq La_4(C_2)_{0.60}Ge_{2.40}$, and La_4Ge_3 demonstrate the existence of a large range of homogeneity $La_4[(C_2)_{1-x}Ge_x]_3$ between the yellow transparent ethenide (4-) La_2C_3 and La_4Ge_3. In the series, the C_2 dumbbells are replaced by Ge atoms, corresponding with the formal charges C_2^{4-}, Ge^{4-}, and La^{3+}. These mixed crystals (Pearson symbol $cI28 \Leftrightarrow 40$) represent a continuous transition between the structure types *cI*40 (Rb_4O_6/Pu_2C_3) and *cI*28 (Th_3P_4). The results are discussed together with the general trends in the members of both structures types. © 1999 Academic Press

Key Words: **lanthanum; dicarbide(4-); germanide(4-); $La_4(C_2)_2Ge$, $La_4[(C_2)_{1-x}Ge_x]_3$ mixed crystals; Ge/C_2 solid solubility.**

INTRODUCTION

Our attempts to find compounds with C–Ge mixed frameworks or clusters in some ternary systems (e.g., K–C–Ge, Ca–C–Ge, Ba–C–Ge, La–C–Ge) failed, but we obtained several new phases. Thus, the compound $Ba_3Ge_4C_2$ contains isolated $[Ge_4]^{4-}$ tetrahedranide as well as C_2^{2-} acetylenide anions (1). Three novel phases were found in the system La–C–Ge, namely $La_5C_2Ge_2$ (*Pbam*, $a = 8.873$ Å, $b = 12.946$ Å, $c = 4.273$ Å; new type) (2), $La_{44}[C_2]_{10}Ge_{26}\square_4$ (*I*4/*mmm*, $a = 11.251$ Å, $c = 17.496$ Å; defect $Ho_{11}Ge_{10}$ type) (2), and $La_4(C_2)_2Ge$ ($I\bar{4}3d$, $a = 8.995$ Å), which is presented here.

EXPERIMENTAL

Synthesis

$La_4(C_2)_2Ge$ was obtained as a minor component from the reaction of the elements La, C, Ge (ratio 6 : 6 : 1) in corundum crucibles enclosed in stainless steel ampoules at 1360 K. The excess carbon is generally amorphous after the reaction, as observed in the system Ba–C–Ge (1).

Crystal Structure Determination

The Laue symmetry, the systematic absences, and the $|E|$ distribution led to the space group $I\bar{4}3d$ (No. 220). The unit cell parameters of the crystal studied were determined from the least-squares refinement of the 2θ values of 61 reflections ($12.7 < 2\theta < 33.8$). The unit cell parameters and the space group indicated that this phase was related to La_4Ge_3 (Th_3P_4 type) as well as to $La_4(C_2)_3$ ($Rb_4(O_2)_3$ type). Thus, the atomic parameters of La_4Ge_3 were used as starting values. The first refinement converged rapidly, but the displacement parameter of Ge indicates a large deficiency in the occupancy of the Ge 12*a* site. After the refinement of SOF(Ge), a series of difference Fourier maps show that carbon C_2 dumbbells center partially the Ge sites (Fig. 1). The parameters of the additional C atoms at 24*d* were further refined on F^2. At this stage, the absolute configuration in respect to the polarity was proven by changing the sign of the *hkl* indices. The $R_w(F^2)$-values for both orientations were 0.061 and 0.064. The former represents then the absolute structure of the studied crystal (Table 2).

As shown in Table 3, the distance d(Ge–La) = 2.873 Å (4×) becomes shorter than the covalent radii sum ($r_{Ge} + r_{La} = 2.91$ Å), which results from the smaller *a*-axis

[1]Present address: Max-Planck-Institut für Chemische Physik fester Stoffe, Bayreuther Straße 40, Haus 16, D-01187 Dresden, Germany.

[2]To whom correspondence should be addressed.

0022-4596/99 $30.00

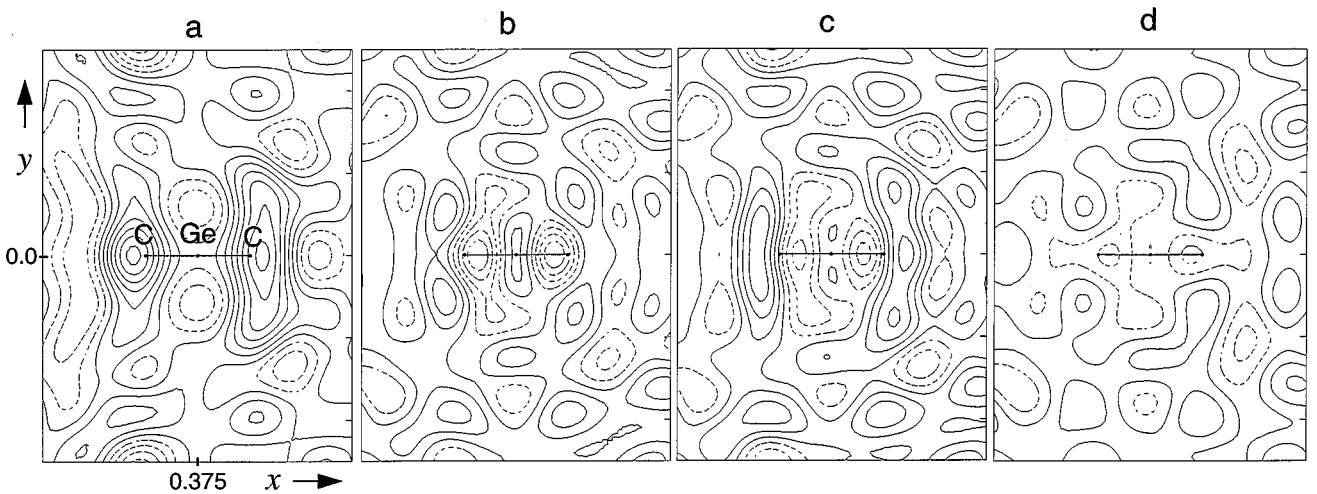

FIG. 1. Difference Fourier sections around the position 12*a* ($\frac{3}{8}\,0\,\frac{1}{4}$) at different stages of the refinements ($\Delta\rho = 0.5$ e/Å^3; broken lines for $\rho < 0$). (a) Position 12*a* occupied by 0.473 Ge with $U_{iso} = 412$ pm^2. (b) Position 12*a* occupied by 0.506 Ge with $U_{11} = 1140$ pm$^2 \gg U_{22} = U_{33} = 255$ pm^2. (c) Split position 24*d* ($x\,0\,\frac{1}{4}$) with $x = 0.3510$ occupied by 0.492 Ge with $U_{iso} = 284$ pm^2. (d) 0.329 Ge at 12*a* and 0.671 C at 24*d* with $x = 0.307$ (see Table 2).

and the x(La) parameter shift (compared with La_4Ge_3). On the other hand, the principal mean square atomic displacements of La (0.0269, 0.0269, 0.0169 Å^2) represents a flattened ellipsoid perpendicular to [111]. Therefore, an alternative solution with a La split position (La* 48*i* in Table 2) was refined and more reliable Ge–La distances were obtained (Table 3, Fig. 4). The *R*-values were similar ($R(F) = 0.033$, $R_w(F^2) = 0.064$ for all data, 10 parameters).

TABLE 1
Selected Crystallographic Data (297 K)

Empirical formula	La_4GeC_4 ($=La_4(C_2)_2Ge$)
Crystal	gray lump ($0.14 \times 0.10 \times 0.03$ mm)
Molar mass	676.27 amu
Space group; formula units	$I\bar{4}3d$ (No. 220); $Z = 4$
Pearson code	$cI28 \Leftrightarrow 40$
Unit cell dimensions	$a = 8.995(1)$ Å, $V = 727.8(1)$ Å^3
d_{calc}	6.172 g·cm^{-3}
Data collection	Siemens P4 four-circle diffractometer, Mo$K\alpha$ ($\lambda = 0.71073$ Å); ω-scan mode; $2\theta \leq 50°$
Data correction	Empirical absorption correction (ψ-scan method), $\mu = 26.95$ cm^{-1}, min. and max. transmission; 0.184, 0.569
Structure refinement	SHELXTL-plus, SHELXL-93 (9 variable parameters) (21, 22)
$N(hkl)$ measured/unique	604/106
$N'(hkl)$ with $I > 2\cdot\sigma(I)$	99
Goodness-of-fit on F^2	1.145
max., min. heights in final $\Delta\rho$ map	1.07, -0.84 e.Å^3
$R(F)$; $R_w(F^2)$	0.030; 0.060 ($I > 2\cdot\sigma(I)$)
$R(F)$; $R_w(F^2)$	0.033; 0.061 (all data)

Relevant crystallographic data are listed in Table 1; the positional and displacement parameters are given in Table 2. Important bond lengths appear in Table 3. Additional material to this paper are available from the Fachinformationszentrum Karlsruhe, D-76344 Eggenstein-Leopoldshafen (Germany), on quoting the deposition number CSD-410866.

RESULTS AND DISCUSSION

$La_4(C_2)_2Ge$ forms gray crystals with metallic luster. The body centered cubic structure ($I\bar{4}3d$; $a = 8.995$ Å; $Z = 4$; Tables 1–4) is a replacement derivative of $La_4(C_2)_3 \triangleq La_2C_3$ ($a = 8.817$ Å) (3) as well as of La_4Ge_3 ($a = 9.3548$ Å) (4) by a partial Ge/C_2 substitution. The compound is one member of mixed crystals $La_4[(C_2)_{1-x}Ge_x]_3$ between $La_4(C_2)_3$ and La_4Ge_3, which represents a continuous transition between the two different cubic structure types *cI*40 (Rb_4O_6 (5) or Pu_2C_3 (6)) and *cI*28 (Th_3P_4 (7)), retaining the $I\bar{4}3d$ symmetry. This may be represented by the Pearson symbol $cI28 \Leftrightarrow 40$ or $cI16 + n$ ($12 \leq n \leq 24$).

The composition $La_4[(C_2)_{0.67}Ge_{0.33(2)}]_3 \triangleq La_4(C_2)_{2.01}Ge_{0.99(6)}$ was refined from the X-ray data. The C–C bond length of about d(C–C) = 1.22(7) Å is consistent with that of $La_4(C_2)_3$ (1.238 Å) and other RE(III) carbides of this type (3) and corresponds with a C=C double bond of a dicarbide(4-) anion.

The La atoms form a 3D framework of condensed La_8 (2, 2, 2, 2) dodecahedra of the bisdisphenoid type, which are centered by Ge atoms or C_2 dumbbells (Fig. 2), remaining empty lanthanum disphenoids around the second *S* point configuration at the 12*b* position. On the other hand, the Ge

TABLE 2
Positional and Displacement Parameters U_{ij}/U_{iso} (in pm^2) for $La_4[(C_2)_{0.67}Ge_{0.33}]_3$ ($La_4(C_2)_2Ge$)

Atom	Site	SOF	x	y	z	U_{11}/U_{iso}	U_{22}	U_{33}	U_{12}	U_{13}	U_{23}
La	16*c*	1	0.05680(8)	x	x	236(4)	U_{11}	U_{11}	− 33(4)	U_{12}	U_{12}
Ge	12*a*	0.33(1)	3/8	0	1/4	161(26)					
C	24*d*	0.67	0.307(4)	0	1/4	224(55)					
[La*	48*i*	0.33	0.0496(15)	0.0692(7)	0.0518(17)	241(8)]					

Note. Displacement factor: $\exp[-2\pi^2(U_{11}h^2a^{*2} + \cdots + 2U_{23}klb^*c^*)]$. Standard deviations are given in parentheses. The alternative split position of the La atoms (La*) is listed at the bottom.

atoms and the centers of the C_2 dumbbells form piles of condensed twisted trigonal antiprisms. The antiprisms share two common faces and are centered by the La atoms (Fig. 3). These piles are further condensed and their arrangement represents the structure of the fourfold rod-packing (8).

A search of the literature reveals the existence of another body centered cubic phase labeled as "$La_5C_{1.5}Ge_3$" ($a = 9.239$ Å (9)). A quantitative analysis of the published powder data shows that $La_5C_{1.5}Ge_3$ is in fact $La_4[(C_2)_{0.20}Ge_{0.80}]_3 \triangleq La_4(C_2)_{0.60}Ge_{2.40}$, which obviously represents a second member of the mixed crystal series. Thus, these findings together suggest the existence of a range of homogeneity $La_4[(C_2)_{1-x}Ge_x]_3$ from $La_4[C_2]_3$ ($x = 0$) to La_4Ge_3 ($x = 1$). The presence of double bonded dicarbide (4-) anions in these compounds corresponds with the distribution of formal quadruple charged C_2^{4-} and Ge^{4-} at the 12*a* position and of La^{3+} at the 16*c* position of the space group $I\bar{4}3d$. It is important to note that in the series of the rare earth carbides RE_2C_3 the europium compound is missing, i.e., there is a preference for the Eu(II)dicarbide(2-) (EuC_2).

The actual members of the mixed crystal series are listed in Table 4. The observed mole fractions x_o fit perfectly the calculated ones from lattice constants (x_a) and unit cell volumes (x_v), respectively: $a/\text{Å} = 8.817 + 0.538\ x_a$ and $V/\text{Å}^3 = 685.4 + 133.3\ x_v$ (Fig. 4). Moreover, the volumes show that the effective volume of Ge^{4-} is by 11.2 Å^3 larger than that of C_2^{4-}. This is also true for other compounds, e.g., the ThGe/ThC_2 pair ($\Delta = 11.0$ Å^3), and corresponds with

TABLE 3
Important Interatomic Distances (in Å)

		$La_4(C_2)_3$	La_4Ge_3	$La_4(C_2)_2Ge$	$La_4^*(C_2)_2Ge$	
La–C	3×	2.686(6)	—	2.807(1)		
	3×	2.886(7)	—	2.89(3)		
	3×	2.973(7)	—	3.06(1)		
	3×	3.925(7)	—	3.92(3)		
–Ge	3×	—	3.056(9)	2.873(1)		
	3×	—	3.437(9)	3.387(1)		
–La	3×	3.63(1)	3.67(1)	3.623(1)		
–La	2×	3.818(1)	4.051(0)	3.895(0)		
–La	6×	4.02(1)	4.40(1)	4.154(1)		
Ge–La	4×	—	3.056(9)	2.873(1)	2.979(7)	
	4×	—	3.437(9)	3.387(1)	3.48(1)	
C–C	1×	1.236(9)	—	1.22(7)	1.22(7)	
–La	2×	2.686(6)	—	2.807(1)	2.74(1) 2.79(1)	side-on
–La	2×	2.886(7)	—	2.89(3)	2.84(3) 2.85(3)	end-on
–La	2×	2.973(7)	—	3.06(2)	2.95(2) 3.07(3)	side-on
–La	2×	3.925(7)	—	3.92(3)	3.84(3) 3.90(4)	

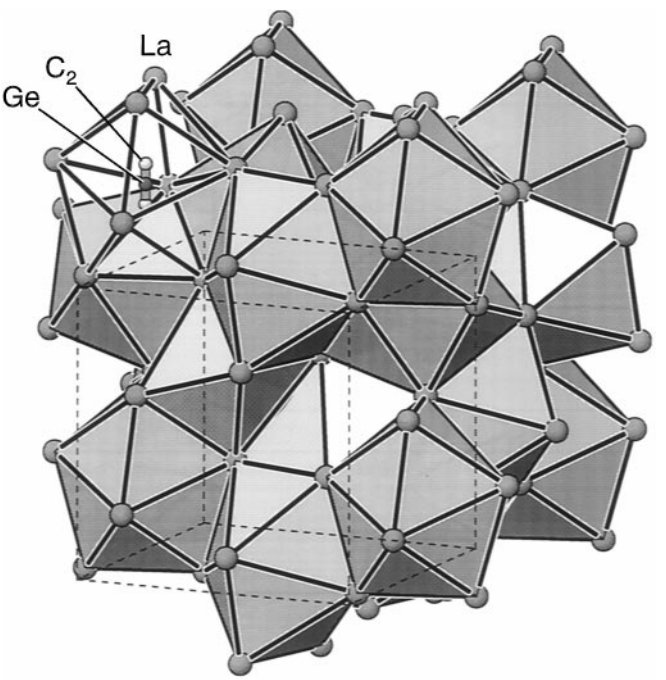

FIG. 2. Structure of $La_4[(C_2)_{0.67}Ge_{0.33}]_3$ showing the framework of condensed La_8 (2, 2, 2, 2) dodecahedra and the orientation of C_2 dumbbells inside one of the La_8 cavities.

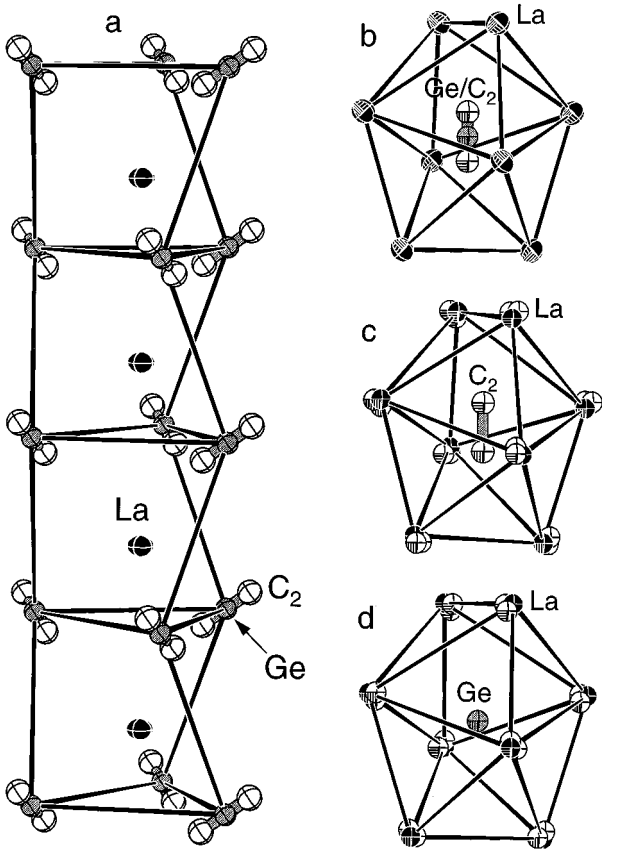

FIG. 3. (a) One of the rods of condensed twisted trigonal antiprisms formed by Ge/C_2 and centered by La. (b) The La_8 cavity around Ge/C_2 with the La average position 16*c*; (c) and (d) short range ordered La atoms (black) around Ge and C_2, respectively, deduced from the La split positions 48*i* in $La_4[(C_2)_{0.67}Ge_{0.33}]_3$ (Table 2). Note the orientations of the C_2 sticks and their side-on as well as end-on coordination by La.

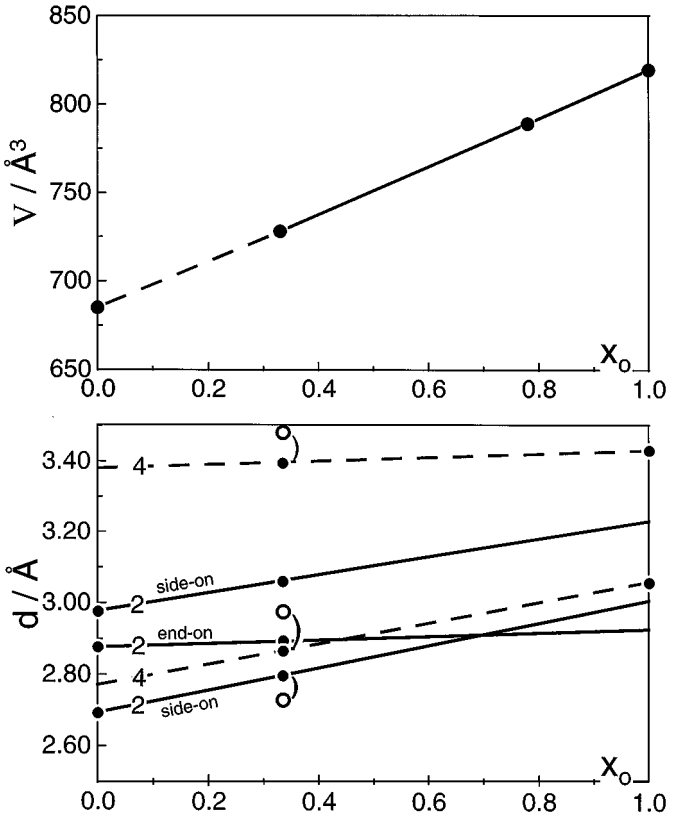

FIG. 4. (top) Linear relation between the unit cell volume and the observed mole fraction x_o in the mixed crystals $La_4[(C_2)_{1-x}Ge_x]_3$. The broken line indicates that the range of homogeneity may be limited (see text). (bottom) Variation of the bond lengths with the mole fraction x in $La_4[(C_2)_{1-x}Ge_x]_3$ calculated from linear relations of a and x(La) with x. Observed values are indicated by dots. Note the shifts of the shortest bond lengths (toward the open circles) by the short range order of La atoms at split positions (see text). d(C–La) continuous lines; d(Ge–La) broken lines.

the difference of the atomic volumes V(Ge)–$2V$(C(diamond)) = 11.29 Å^3.

The statistical distribution of spherical atoms and of dumbbells with fixed orientations at the same crystallographic position leads to some discrepancies in the coordination and bond lengths. This is best seen, e.g., by analyzing a hypothetical mixed crystal $MnS_2/MnSe$ (pyrite structure vs rock salt structure). In the present structure, the positional parameter x(La) defines the shape of the coordination polyhedron around the position 12*a* (and 12*b*) of the space group $I\bar{4}3d$. In the range $0 \le x(\text{La}) \le 0.125$, the substructure of the La atoms is completely changed from a I_2 point configuration (2^3 *bcc* unit cells, $I_2m\bar{3}m$, CN 8 + 6) to the famous Y^{**} point configuration of the space group $Ia\bar{3}d$ (CN 3 + 2 + 6 + 6) (for the distances see Fig. 6). The coordination polyhedron around the position 12*a* changes from a (2, 2) disphenoid (x(La) = 0) to a (2, 2, 2, 2) bisdisphenoid (x(La) = 0.0833) and then to a (2, 4, 2) polyhedron (x(La) = 0.125), whereas the polyhedron around the empty 12*b* position changes from a flattened to an elongated (2, 2) disphenoid and then to a (2, 4, 2) polyhedron.

The most regular (2, 2, 2, 2) dodecahedron is achieved with x(La) = 1/12 = 0.0833 (Fig. 5), but with this parameter the Madelung energy MAPLE (10) would be lowest (constant volume) because of the three short d(La–La) distances

TABLE 4
Unit Cell Dimensions (at 297 K) and Mole Fractions x for $La_4[(C_2)_{1-x}Ge_x]_3$

Phase	a/Å	V/Å^3	x_o	x_a	x_V	x(La)	(ref.)
$La_4[C_2]_3$	8.817(5)	685.4	0	0	0	0.0504	(3)
$La_4[(C_2)_{0.67}Ge_{0.33}]_3$	8.995(1)	727.8	0.33	0.33	0.32	0.0568	this work
$La_4[(C_2)_{0.20}Ge_{0.80}]_3$	9.239(5)	788.6	0.80	0.78	0.77	—	(9)
$La_4[Ge]_3$	9.3548(3)	818.7	1	1	1	0.0645	(4)

Note. x_o from the X-ray refinement or chemical analysis. x_a and x_V from linear relations of the lattice constants a and the unit cell volumes V (see text).

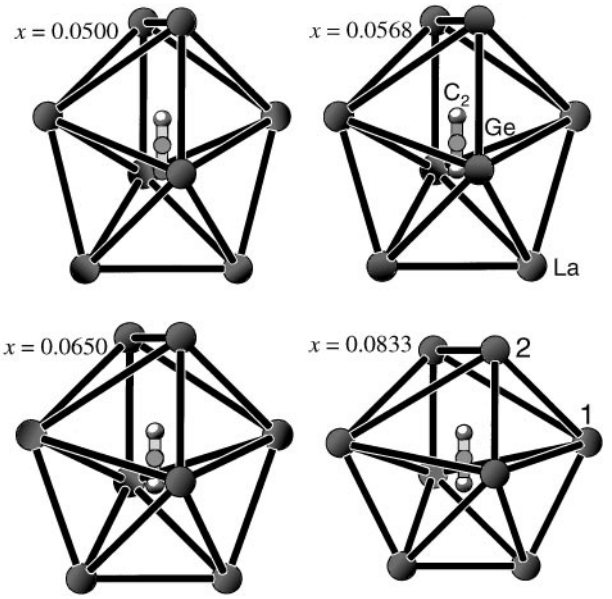

FIG. 5. Shape of the La_8 dodecahedron around Ge/C_2 changed by the La positional parameter (average) $x(16c)$ in the real structure of $La_4[(C_2)_{1-x}Ge_x]_3$ (mole fraction $0 \le x_o \le 1$); the most regular polyhedron ($x = 0.0833 = 1/12$) is never reached.

(Fig. 6). Therefore, the parameter shift to lower x values is forced by MAPLE but blocked by the Ge–La interatomic Born repulsion at about 3 Å (Fig. 6). This is true in all real Th_3P_4 type structures, where the parameter of about 0.065–0.073 (11) yields an elongated and twisted (2, 2, 2, 2) dodecahedron around 12*a* with four shorter and four longer distances: $((\frac{3}{8}\,0\,\frac{1}{4}) - (xxx + \frac{1}{4}\frac{1}{4}\frac{1}{4}))$ and $((\frac{3}{8}\,0\,\frac{1}{4}) - (xxx))$, respectively (Figs. 5, 6).

In the *cI*40 structure of Rb_4O_6 (5, 12) and the dicarbides M_4C_6 (3, 6), the positional parameter of the metal atoms is changed significantly to lower values, $x(16c) \approx 0.05$ (Fig. 6). The resulting M_8 polyhedron stretches out in order to envelope the X_2 dumbbells by 2×2 end-on and $2 + 2$ side-on ligands (Figs. 5 and 6). In the mixed crystals, the lattice constant a as well as the parameter x(La) is changed (Table 4), which leads to very short Ge–La distances with decreasing mole fraction x, indicated by broken lines in Fig. 6. However, the small shifts of the La atoms from the $16c(xxx)$ position to the three split positions around the [111] axis allows the development of a short range order structure, which avoids this complication. The shortest Ge–La distance is changed from 2.873 to 2.979 Å in the $x = 0.33$ crystal (Tables 2, 3). This is demonstrated in Figs. 3, 4, and 6. Close to $x = 0$ this Ge–La distance would be about 2.78 Å, and we are unsure that the necessary larger shift of the La atoms is possible, because on the other hand some C–La distances become too short. Thus, it may be that the solid solubility of Ge in $La_4(C_2)_3$ is limited, and perhaps $La_4(C_2)_2Ge$ was formed as the boundary phase at $x \approx 0.33$ under the preparation conditions (broken line in top of Fig. 4). The increasing C–La distances with mole fraction x allows a tumbling of the C_2 dumbbells around [100]. This should be proven by further studies.

We recommend the excellent work done by *Helms* and *Klemm* in 1939 (5), who derived the structure of Rb_4O_6 (Cs_4O_6) from the X-ray powder pattern, showing that $x(Rb) = 0.05$ is far from $x = 1/12 = 0.0833$ (given for P in Th_3P_4 by Meisel (7)) and discussing in detail the optimal shape of the Rb_8 cavity to envelope the O_2 dumbbells oriented along [100]. Furthermore, they explained the black color of Rb_4O_6 (in contrast to that of the neighboring phases Rb_2O_2 and RbO_2) with the presence of O_2^{1-} and O_2^{2-} anions in the ratio 2 : 1, in accordance with the magnetic moment. Unfortunately, *Helms* and *Klemm* did not claim a new structure type for this novel *cI*40 structure but called it an *anti*-Th_3P_4 derivative (*cI*28) with O_2 dumbbells replacing single atoms (cf. the pair FeS_2/NaCl). Recently, *Jansen* and *Korber* (12) established the structure by X-ray single crystal studies and more recently with elastic and inelastic neutron scattering (13), verifying with the latter the presence of both kinds of anions O_2^{1-} and O_2^{2-}. The M atom at 16*c* shows a flattened displacement ellipsoid (12) on the same order of that in $La_4(C_2)_2Ge$, which indicates again a short range order to fit the coordination of the two different O_2 dumbbells.

The complete characterization of the compounds $Ba_3Ge_4C_2$ (1), $La_5C_2Ge_2$ (2), $La_{44}[C_2]_{10}Ge_{26}\square_4$ (2), and $La_4(C_2)_2Ge$ has shown again that they do not contain C–Ge fragments, but contain isolated C_2 dumbbells together with Ge_n clusters or Ge atoms. On the other hand, we succeeded in obtaining C–Sn as well as Ge–Sn mixed covalent frameworks in the K–C–Sn and K–Ge–Sn systems, namely the mixed clathrates-I $K_8C_nSn_{44-n}$ ($n < 22$) and $K_8Ge_nSn_{44-n}$ ($0 < n < 44$), respectively (2). This is important in relation to the fruitless search for solid state compounds with C–Ge bonds. The present eletronegativity scales (14, 15) shows that $\Delta\chi$(C–Ge) is lowest in the combinations of carbon with the series of the E14 elements: $\Delta\chi$(C–Ge) < $\Delta\chi$(C–Si, Sn, Pb). Especially from Sanderson's scale (15) follows $\chi(C) - \chi(Ge) \approx 0$. Therefore, in addition to the homoatomic bonding interactions, one expects the lowest polar contribution in the bond energy E_b in this combination of elements:

$$2E_b(C\text{–}Ge) \approx E_b(C\text{–}C) + E_b(Ge\text{–}Ge)$$

$$2E_b(C\text{–}Si, Sn, Pb) > E_b(C\text{–}C) + E_b(Si\text{–}Si, Sn\text{–}Sn, Pb\text{–}Pb).$$

This also means that the C–Ge bonds in the numerous molecules will not be stable in thermodynamically governed equilibria with respect to the homoatomic bonds of the educts.

The finding that $La_5C_{1.5}Ge_3$, characterized by X-ray powder methods, is in fact $La_4[(C_2)_{0.20}Ge_{0.80}]_3$ and belong

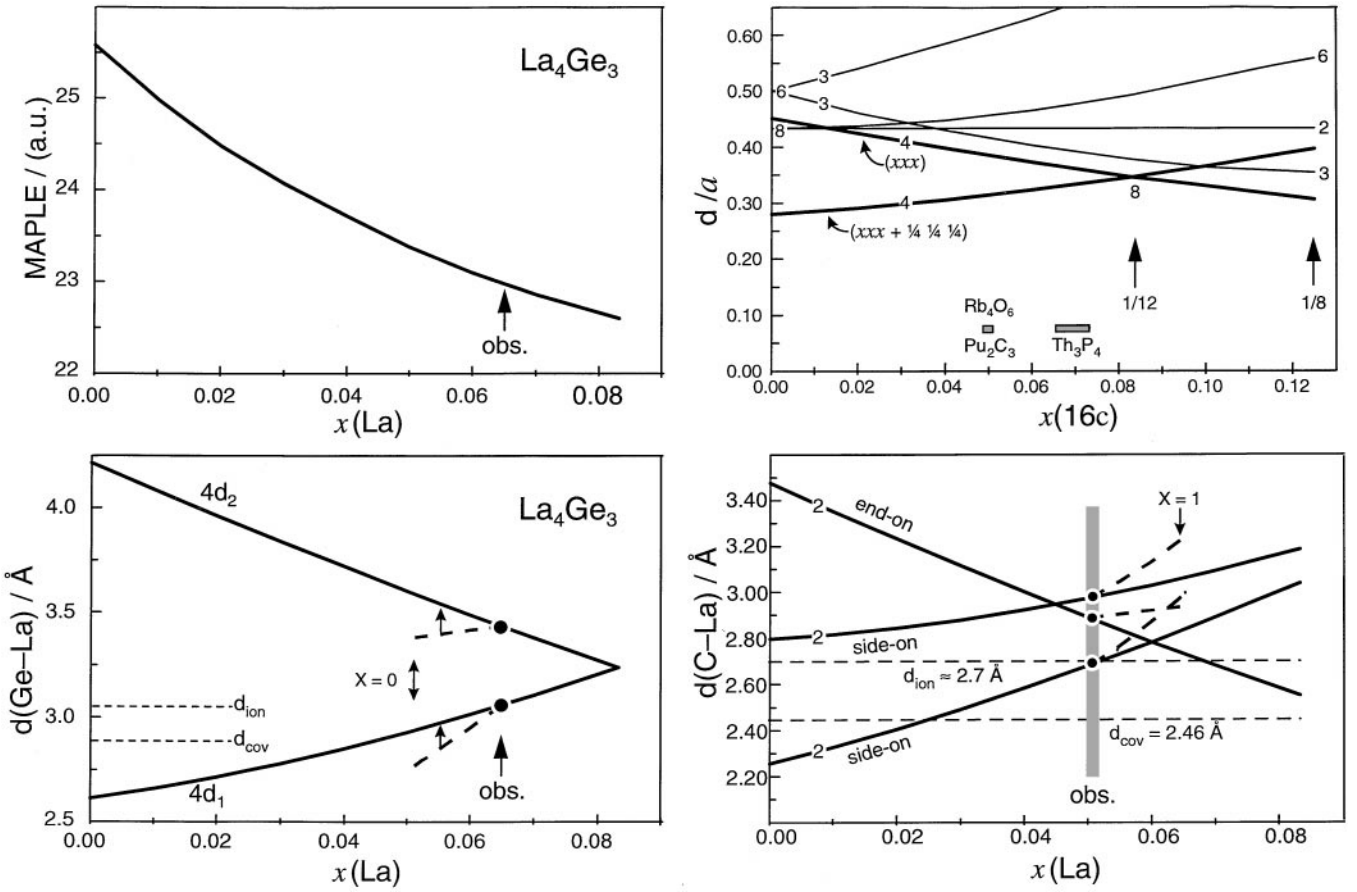

FIG. 6. (top left) Lattice energy MAPLE (in a.u.) as a function of the positional parameter x(La) in La_3Ge_4 with constant volume. (La^{3+}, Ge^{4-}; MAPLE (in eV) values by multiplication with 14.400). (bottom left) Variation of the Ge–La distances in the La_3Ge_4 structure (V = const.) with the positional parameter x(La) (dots = observed values). The variations for the mixed crystals in the range of homogeneity $0 \le x \le 1$ are represented by bold broken lines. The shifts toward suitable distances in the short range order structure are indicated by small arrows (see text). (top right) Variations of the relative distances d/a with the positional parameter x(16c) in the Th_3P_4 type structure ($cI28$). (Minority component at 12a ($\frac{3}{8}\,0\,\frac{1}{4}$) and majority component at 16c (xxx) of the space group $I\bar{4}3d$ (No. 220); bold lines = d(12a − 16c) and thin lines = d(16c − 16c) together with the number of equivalent distances). The regions of observed x-values for the Th_3P_4 and Rb_4O_6 (Pu_2C_3) families are also indicated. (bottom right) Variation of C–La distances with the positional parameter in pure $La_4(C_2)_3$. The bold broken lines show the changes in the $La_4[(C_2)_{1-x}Ge_x]_3$ range of homogeneity (not linear because of the combined variation of a and x(La) with the mole fraction x).

to the mixed crystal series discussed above (Table 4) suggested that other ternary carbides might belong to analogous families of mixed crystals. According to the last edition of Pearson's Handbook (16), not only the large group of RE(III) dicarbides(4-) $RE_4(C_2)_3 \triangleq RE_2C_3$ together with Th_2C_3 belong to the $cI40$ structure type of Pu_2C_3 (Rb_4O_6), but also a series of miraculous ternary phases, looking like a result of an "exploded pharmacy:" $C_{15}M'Th_9$ (M' = Er, Ce, Dy, Gd, Ho, Lu, Sc, Nd, Pr, Tb); $C_{27}Th_6Y_{14}$; C_7La_4Th; $C_{27}M'_2M_{18}$ (M = Y, La; M' = Si, Ge, Sn, Th Nb, Ru, Ti); $C_{29}M'_2Y_{18}$ (M' = Bi, Cr, Mo, V, W, Zr); $C_{29}U_3Y_{17}$.

A closer look at the original data shows that most of the incredible formulae arise from the multiplication by "appropriate" factors done by the book authors in order to yield integer numbers, regardless of the necessary 40 atoms per unit cell. Going back to the original data, a complete analysis of the unit cell volumes has been done with the help of a renewed system of "volume increments" per atom (17), which allows the calculation of the volumes of nitrides, phosphides, carbides, silicides, and germanides of the rare-earth metals and thorium within 1–2 percent (18). The results are: All phases were originally written as $C_3(M'_xM_{1-x})_2$ or $C_{1.45}M'_xM_{1-x}$ or $C_{1.35}M'_xM_{1-x}$ (M = Y, La, Th). This leads in a $cI40$ unit cell to $C_{24}(M'_xM_{1-x})_{16}$ or $C_{23.2}(M'_xM_{1-x})_{16}$ or $C_{21.6}(M'_xM_{1-x})_{16}$ in most cases with $0 \le x \le 0.1$ and in a few examples up to $x = 0.3$. This type of "alloying" seems to be typical for the chase after materials with special properties, e.g., superconductivity (see below) and, indeed, some phases are reported

as new high T_c-superconductors as early as 1969 (19). The chemical composition only reflects the synthetical input and, therefore, the differences in the nominal carbon content are not serious. The analysis of the volumes shows (18) that the upper limit is the mole fraction x is mostly lower and in some cases $x = 0$.

The three phases $C_{27}M'_2Y_{18}$ with $M' =$ Si, Ge, Sn are of special interest in the context of this paper. Their cell volumes (566.0, 568.9, 560.1 Å^3) are *larger* than that of $C_{24}Y_{16}$ (559.0 Å^3). For the cases with $M' =$ Si, Ge, the results are in contrast to the volumes V(Y) vs V(Si), V(Ge) (26.4 Å^3 vs 20.02, 22.64 Å^3). Therefore, silicon and germanium cannot replace yttrium but must replace the smaller C_2 dumbbells (10.6 Å^3), corresponding with the composition $Y_{16}[(C_2)_{1-x}M'_x]_3 \triangleq Y_4[(C_2)_{1-x}M'_x]_3$ with $x = 0.08$ in both cases. Thus, it seems that the phases with Si and Ge belong to mixed crystal series like $La_4[(C_2)_{1-x}Ge_x]_3$. The Sn phase may also exist, but the appropriate Sn position can hardly be predicted because of the different atomic volumes of α-Sn (33.80 Å^3) and β-Sn (26.97 Å^3).

Additionally, some curiosities were noticed in this study. From the volumes, it follows straightforwardly that "Sc_2C_3" (*cI*40) is definitely Sc_4C_3 (*cI*28; Th_3P_4 type). The composition C_6ThY (16) was calculated from the original $C_3(Th_{1-x}Y_x)_2$ with $x = 0.5$ by applying the famous tailor's rule "two times cut but even more too short."

Simon (20) recently explained the crucial role of the C_2-π^* states for the superconductivity of dicarbides and the importance of 2-electron steps (C_2^{4-}, C_2^{6-}). Moreover, it seems that the simultaneous interaction of the M atoms as *side-on* and *end-on* ligands is another important detail in the dicarbide structures. The analysis of volumes and unit cell parameters has shown that the ratios M'/M as well as $(M' + M)/C$ are the weakest data. Furthermore, mixed crystals of the $M_4[(C_2)_{1-x}M'_x]_3$ type demonstrate the possibility of substituting C_2 dumbbells by single atoms. In other words, one has to expect the presence of, e.g., methanide C^{4-} anions together with dicarbide(4-) and dicarbide(6-) anions in these compounds. This is important in the discussions on the optimal ratios $\Sigma n_e/C_2$ of transferred electrons to the C_2 dumbbells corresponding with the T_c maximum of superconductors (20). Finally, it should be pointed out here that the electron transfer in the black Rb_4O_6 and Cs_4O_6 compounds (5, 12) corresponds exactly with that in Th_4C_6 ($C_2^{5.33-}$ isoelectronic with $O_2^{1.33-}$).

ACKNOWLEDGMENT

We thank the *Fonds der Chemischen Industrie* for financial support.

REFERENCES

1. J. Curda, W. Carrillo-K. Cabrera, A. Schmeding, K. Peters, M. Somer, and H. G. von Schnering, *Z. Anorg. Allg. Chem.* **623,** 929 (1997).
2. J. Curda, W. Carrillo-Cabrera, K. Peters, M. Baitinger, Yu. Grin, and H. G. von Schnering, to be published.
3. (a) M. Atoji and D. E. Williams, *J. Chem. Phys.* **35,** 1960 (1961). (b) M. Atoji, K. Gschneidner, A. H. Daane, R. E. Rundle, and F. H. Spedding Jr., *J. Am. Chem. Soc.* **80,** 1804 (1958). (c) F. H. Spedding Jr., Gschneidner, and A. H. Daane, *J. Am. Chem. Soc.* **80,** 4499 (1958).
4. (a) A. M. Guloy and J. D. Corbett, *Inorg. Chem.* **32,** 3532 (1993). (b) D. Hohnke and E. Parthé, *Acta Crystallogr.* **21,** 435 (1961).
5. A. Helms and W. Klemm, *Z. Anorg, Allg. Chem.* **242,** 201 (1939). Rb_4O_6 was the first identified member of the *cI*40 structure family, which for unknown reasons is named the Pu_2C_3 type.
6. W. H. Zachariasen, *Acta Crystallogr.* **5,** 17 (1952).
7. K. Meisel, *Z. Anorg. Allg. Chem.* **240,** 300 (1939).
8. M. O'Keeffe and S. Andersson, *Acta Crystallogr. A* **33,** 914 (1977).
9. I. Mayer and I. Shidlovsky, *J. Appl. Crystallogr* **1,** 194 (1968).
10. R. Hoppe, *Angew. Chem. Int. Ed. Engl.* **5,** 95 (1966).
11. Parameters of refined structures without "most reliable" values.
12. M. Jansen and N. Korber, *Z. Anorg. Allg. Chem.* **598/599,** 163 (1991).
13. M. Jansen, N. Korber, and R. Hagenmayer, to be published.
14. J.Emsley, "The Elements," 3rd ed., Clarendon Press, Oxford, 1998.
15. R. T. Sanderson, "Polar Covalence," Academic Press, New York, 1983.
16. P. Villars and L. D. Calvert, "Pearson's Handbook of Crystallographic Data for Intermetallic Phases," 2nd ed. *ASM International*, *Metals Park*, *Ohio*, 1991.
17. W. Biltz, "Raumchemie de festen Stoffe," Leopold Voss Verlag, Leipzig, 1934.
18. H. G. von Schnering and W. Carrillo-Cabrera, to be published.
19. M. C. Krupka, A. L. Giorgi, N. H. Krikorian, and E. G. Szklarz, *J. Less-Comm. Met.* **19,** 113 (1969).
20. A. Simon, *Angew. Chem. Int. Ed. Engl.* **36,** 1789 (1997).
21. G. M. Sheldrick, Program Package SHELXTL-plus. Release 4.1. Siemens Analytical X-Ray Instruments Inc., Madison, WI, 1990.
22. G. M. Sheldrick, SHELXL-93. Program for Refining Crystal Structures, University of Göttingen, Germany, 1993.